

Three-Dimensional Modeling of Human Placental Terminal Villi

Romina Plitman Mayo^{a,b}, D. Stephen Charnock-Jones^{a,c}, Graham J. Burton^a, Michelle L. Oyen^{a,b}

^a*Centre for Trophoblast Research, Department of Physiology, Development and Neuroscience, University of Cambridge, Cambridge, UK*

^b*Nanoscience Centre, Department of Engineering, University of Cambridge, Cambridge, UK*

^c*Department of Obstetrics & Gynaecology, University of Cambridge, Cambridge, UK*

Abstract

Introduction: Placental transport is the main factor affecting the health and development of the fetus. Due to the placenta's geometrical and mathematical complexity, the structure-function relations of placental terminal villi have not been successfully modeled. Hence, a novel modeling approach is proposed.

Methods: Computational models of four different specimens were generated from the three dimensional reconstruction of confocal laser scanning microscopic image stacks. To evaluate the capabilities of the proposed methodology, stationary oxygen diffusion transport was calculated in the terminal villus volumes.

Results: The reconstructions automatically provided the spatial arrangement of the fetal capillaries inside the terminal villi. The surface and volume ratios between the fetal capillaries and the villus were also calculated, and the effects of model parameters on the placental diffusive capacity were assessed by parametric analysis.

Discussion: The potential of three-dimensional reconstructions combined with finite element analysis as a research tool for the human placenta was tested. The methodology herein could serve in the future as a simulation platform for complicated *in vivo* and *in vitro* scenarios.

Keywords: Oxygen Transport, Placenta, Terminal Villi, Confocal Laser Scanning Microscopy, Diffusion Analysis

1. Introduction

Placental oxygen transport is believed to be the most important function of the human placenta. At the smallest branches of placental villous trees, diffusive transport takes place due to concentration gradients that arise between the outer surface of the trophoblast layer and the inner surface of the fetal capillary endothelium [1]. These terminal villi are believed to be the most important sites for gas exchange due to their thin barriers between the maternal and fetal bloodstreams [2]. Therefore, their structure-function relations are of great interest to placental physiologists.

Histological methods have been very popular for the assessment of terminal villous geometry since they provide an approximation of the complex three-dimensional (3D)

11 structure [3–5]. However, the published data are sparse and inconsistent, mainly due to the
12 different investigation and fixation procedures employed. The 3D architecture of the villus
13 was first visualized and quantified using scanning electron microscopy and vascular corrosion
14 casts, [6, 7] which allowed for easier and more exact approaches than histology. Currently,
15 3D imaging techniques such as X-ray microcomputed tomography (microCT) and confocal
16 laser scanning microscopy (CLSM) are providing new methods for studying vessel alterations
17 in humans and animals. The 3D fetoplacental vascular bed of normal and pathological
18 human placentae has been investigated using microCT [8, 9]; however, its resolution is not
19 enough for the acquisition of a detailed structure of the terminal villi. CLSM has provided
20 unique information regarding the 3D spatial arrangement of microvascular beds in normal
21 and pathological placentae, during the first [10] and third [11, 12] trimesters. Volumetric
22 reconstructions of CLSM images could provide useful insights if combined with mathematical
23 modeling.

24 Mathematical models of placental exchange function were initially described more than 40
25 years ago [2, 13]. The different modeling approaches can be classified into two broad groups:
26 based on experimentally obtained geometry and on parametrized geometry. The first group
27 is mostly composed by studies that adapted the two-dimensional (2D) morphometric model
28 developed for the gas exchange in the lungs [14] to the placenta [3, 5, 15–18]. A different
29 methodology was employed by Gill et al. [2], who used digital photomicrographs to extract
30 the 2D geometry of the villi and their respective capillaries. The extent of diffusional screening
31 in placental villi was then numerically calculated. Their work is pioneering and has the
32 advantage that it can be performed in multiple villi simultaneously. Similarly, Chernyavsky
33 et al. [19] estimated the distribution of villous branches in the intervillous space, and solute
34 transport was modeled. However, when experimental data are not available, such as for
35 the branching villus trees, the only way of solving a more comprehensive mathematical
36 model is by simplifying the geometry to known geometrical shapes - *e. g.* tubes and ovals.
37 These type of studies form the second and smallest group of placental modeling [20–22].
38 Thus, most of the studies performed on the oxygen transport in the human placenta have
39 successfully modeled it in 1D and 2D, but those who attempted to do so in 3D were required
40 to simplify the geometrical structure. For a detailed review on models of oxygen transport in
41 the placenta the reader is referred to Serov et al. [23].

42 In the current study, three-dimensional reconstructions of terminal villi and their capillary
43 beds are combined with finite element (FE) analysis to test their potential as an investigative
44 tool. The technique is tested by solving stationary oxygen diffusive transport. This approach
45 accounts for specimen-specific geometry where the contribution of the villous membrane and
46 fetal capillary variability is directly incorporated, while their effect in 3D is quantified and
47 visualized. It also provides the opportunity to investigate in detail the structure-function
48 relation in the terminal villi.

49 2. Material and Methods

50 2.1. Specimen Preparation

51 A fresh healthy placenta delivered by Cesarean section at term was obtained at the
52 Department of Obstetrics & Gynaecology in Addenbrooke’s Hospital for perfusion fixation
53 [24], with ethical permission and informed written consent. Two undamaged and clot-free
54 lobules suitable for perfusion were identified and the amnion was removed from the chorionic
55 plate above these. The chorionic artery supplying each lobule was cannulated and the
56 draining vein was cut to allow perfusate flow. Fetal blood was cleared from the lobules
57 with phosphate buffered saline (PBS). The lobules were then fixed by perfusion with 10%
58 formalin (20 min) followed by removal with PBS (an additional 20 min). The vessels were
59 perfused with PBS containing green fluorescein isothiocyanate (FITC) conjugated Ulex lectin
60 (FL-1061, Vector Laboratories Peterborough, Cambridgeshire, UK) that has an excitation
61 and emission maximum wavelength of 495 nm and 515 nm respectively. Once the vessels
62 were filled, the solution was left in place for 30 min and then removed by flushing with PBS.
63 The two lobules were processed at 2 different perfusion pressures: 100 mmHg (specimen
64 1 and 2) and 30 mmHg (specimen 3 and 4) representing the extremes of the physiological
65 pressures [25]. Intermediate villi with small clumps of terminal villi attached were dissected
66 with needles and incubated for 10 minutes in DiI (D-282, Life technologies, CA, USA) to
67 stain the villous membranes (excitation maxima wavelength of 549 nm and emission maxima
68 wavelength of 565 nm).

69 The specimens were scanned using a Leica SP2 CLSM (Leica Microsystems, Wetzlar,
70 Germany) with an x25, 0.95NA objective lens. Based on the quality of the images (which is
71 a function of the quality of the perfusion), four terminal villi were selected for quantitative
72 analysis. For each sample, image stacks with a resolution of $0.277 \mu\text{m}^2 \times 2 \mu\text{m}$ were
73 automatically generated.

74 2.2. Geometry Reconstruction

75 The CLSM data were imported into 3DSlicer [26], an open-source software for image
76 analysis. The stacks were converted to grayscale images and the geometries of interest
77 were automatically detected by the thresholding method, where each grayscale image was
78 transformed into a binary one [27]. Thereafter, manual cleaning based on human interpre-
79 tation was needed to remove image artifacts and define unclear boundaries; for example,
80 when two close but obviously different capillary segments appear merged within the same
81 boundary they are manually disconnected and the resulting gap equals the pixel size (0.277
82 μm). For better processing, a Gaussian blur smoothing algorithm [27] was applied to further
83 clean and reduce noise. Due to the lack of information regarding the material properties
84 (diffusion coefficients) of the trophoblast epithelium, basement membrane, connective tissues
85 and capillary endothelium, they were modeled together as a single entity called the villous
86 membrane. Three-dimensional triangulated meshes were generated from the segmented
87 stacks with the help of an interpolation algorithm [28] and converted into point clouds (a
88 collection of points that describes the surface of a given shape) by employing an in-house
89 code that extracts the triangle vertices. The solid bodies (volumetric geometry) which mimic

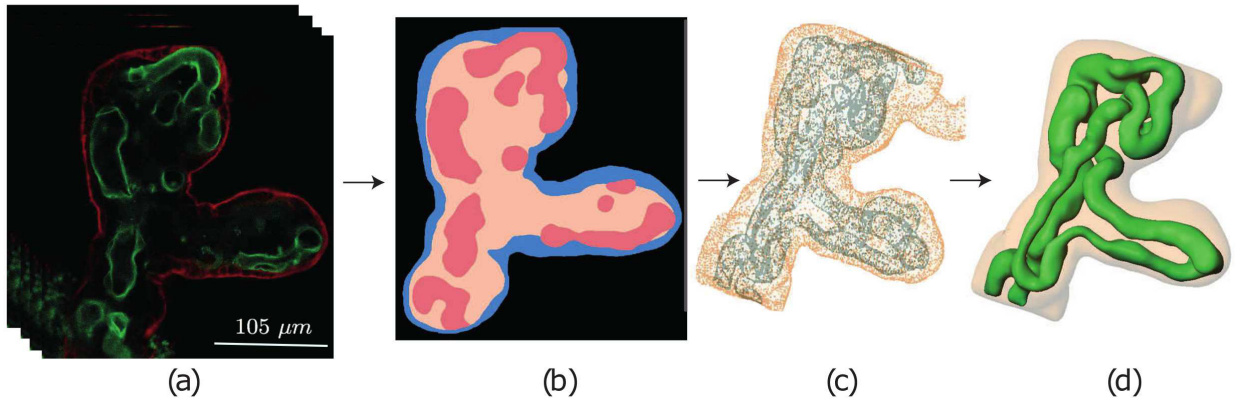


Figure 1: Schematic flow chart for the reconstruction of 3D geometries from CLSM stacks. (a) Typical 2D CLSM slice where the trophoblastic layer (red) and the fetal capillaries (green) are visible, (b) Typical 2D label-map with colors for the different tissues: blue for the trophoblastic membrane, beige for the stroma and pink for the fetal capillaries, (c) Point cloud of the villi and fetal capillary surfaces and (d) 3D Solid bodies.

90 the specimen specific terminal villi and fetal capillaries were automatically generated in
 91 SolidWorks-2013 software (SolidWorks Corporation, MA, USA) by employing the PointCloud
 92 function. The overall 3D reconstruction process is schematically shown in Figure 1.

93 The microscopic size of the samples challenges the verification of the geometries. Therefore,
 94 a methodology that enables the estimation of the reconstruction accuracy was developed.
 95 Four $r = 90 \mu\text{m}$ and three $r = 4 \mu\text{m}$ spheres were scanned with equal parameters as the
 96 villous specimens, but with 3 different slice thicknesses. The spheres were reconstructed and
 97 analyzed. The data indicated that the precision of the geometrical reconstruction mostly
 98 depends on the slice thickness. For the given geometries, a 1% error is expected in each
 99 direction (x, y, z).

100 2.3. Computational Model

101 The 3D solid bodies were imported and implemented using the commercial FE solver
 102 COMSOL Multiphysics 5.2 (COMSOL, Inc., Burlington, MA, USA). The villous membrane
 103 and fetal capillaries were treated as different domains to allow for different boundary
 104 conditions. These two domains were meshed separately with continuity across the boundary,
 105 by the COMSOL automesh. Due to the volume and complexity of each specimen, the
 106 size of the meshes differed greatly ranging from 430,000 to 825,000 tetrahedral elements. A
 107 typical mesh sensitivity procedure [29] in which the meshes are refined and the convergence
 108 of the results is checked was performed. Minimum element size was less than minimum
 109 thickness to reduce numerical errors.

110 A passive oxygen transport problem was considered to evaluate the capabilities of the
 111 presented method. The oxygen is assumed to diffuse through the villous membrane following
 112 Fick's second law of diffusion, Eq. 1, which states that the oxygen volume flow (with time t)

113 across a membrane is related to its physical dimensions (x, y, z), the driving concentration
 114 gradient, $\nabla\mathbf{C}$, and the diffusion coefficient, D .

$$\frac{\partial\mathbf{C}}{\partial t} = D\left(\frac{\partial^2\mathbf{C}}{\partial x^2} + \frac{\partial^2\mathbf{C}}{\partial y^2} + \frac{\partial^2\mathbf{C}}{\partial z^2}\right) = D\nabla^2\mathbf{C} \quad (1)$$

115 The oxygen concentration at the villous membrane corresponds to the maternal blood
 116 concentration, which varies according to the position of the terminal villus in the intervillous
 117 space and the proximity to other terminal villi. However, since both parameters are unknown
 118 a constant oxygen concentration surrounding the villi ($C_{villi} = 1 \cdot 10^{-9} \text{ mol/m}^3$) was assumed.
 119 Since it is not possible to determine from 2D CLSM images which capillaries carry oxygenated
 120 blood and which carry deoxygenated blood, all fetal capillaries were treated as carrying
 121 arterial deoxygenated blood and thus acting as perfect sinks for oxygen ($C_{capillaries} = 0$
 122 mol/m^3). Different values of the concentration gradient between the villi and capillary
 123 surfaces were tested.

124 To the best of the authors' knowledge, the diffusion coefficient of oxygen in placental tissue
 125 has not been directly measured. Some investigators have assumed the diffusion coefficient of
 126 the villous membrane to be similar to the oxygen diffusivity in plasma [2] and others to the
 127 diffusion coefficient of oxygen in water [15]. Due to the lack of data, a parametric evaluation
 128 of the diffusion coefficient was also performed.

129 There was no account for oxygen uptake by the villous stroma, nor the local pressure
 130 variations and other forces due to the maternal and fetal circulations. Stationary oxygen
 131 diffusion was assumed since the time for maternal blood to travel through the intervillous
 132 space (10-20 s) is considerably longer than the time for oxygen to diffuse into a villus (order
 133 of seconds) [1]. The solver run time ranged between 40 and 250 seconds.

134 Transport efficiency of the terminal villi has been suggested as the ratio between oxygen
 135 flux (Eq. 2) and capillary cross sectional area [2]. However, the area across which oxygen
 136 reaches the fetal bloodstream from the villous membrane is the surface area rather than the
 137 cross-sectional area of the capillaries. Therefore, a new oxygen transport efficiency which
 138 allows for geometric variability to be taken into account is proposed (Eq. 3).

$$J = -D\nabla\mathbf{C} \quad (2)$$

$$E = \frac{J}{V_{cap}} \quad (3)$$

139 The flux magnitude refers to the volumetric integration of the diffusive flux magnitude
 140 over the villous membrane, representing the amount of oxygen that will be absorbed by the
 141 capillaries and V_{cap} refers to the capillary volume.

142 3. Results

143 3.1. Geometrical Reconstructions

144 Figure 2 shows the reconstructed geometries of the four specimens from the CLSM stacks,
 145 together with cross sectional slices for better visualization. Examples of the vasculo-syncytial

Table 1: Geometrical details of the villi and capillary beds.

Parameter	Specimen 1	Specimen 2	Specimen 3	Specimen 4
Fixation Pressure [mmHg]	100	100	30	30
Villous Volume ^a [μm^3]	$2.59 \cdot 10^6$	$2.25 \cdot 10^6$	$3.06 \cdot 10^6$	$3.21 \cdot 10^6$
Capillary Volume [μm^3]	$7.27 \cdot 10^5$	$5.58 \cdot 10^5$	$6.40 \cdot 10^5$	$6.79 \cdot 10^5$
Volume Fraction ^b [%]	28	25	21	21
Villous Surface Area [μm^2]	$1.23 \cdot 10^5$	$1.28 \cdot 10^5$	$1.59 \cdot 10^5$	$1.35 \cdot 10^5$
Capillary Surface Area [μm^2]	$1.29 \cdot 10^5$	$1.05 \cdot 10^5$	$1.24 \cdot 10^5$	$1.21 \cdot 10^5$
Surface Fraction ^c [%]	105	82	78	89

^a Includes capillary volume.

^b Capillary to villous volume fraction.

^c Capillary to villous surface fraction.

146 membranes, usually defined as localized areas where the membrane separating the maternal
 147 and fetal blood streams are particularly thin [30], are indicated with arrows. It can also
 148 be observed that the capillaries have variable diameters, follow a sinuous course and form
 149 different types of loops.

150 Parameters of interest are directly obtained from the reconstructions and summarized in
 151 Table 1. Smaller values of the perfusion pressure resulted in a decrease of the volume ratio,
 152 defined as the ratio between the capillary volume to that of the villus. The surface area ratio
 153 (Eq. 4) between the capillaries and the villous membrane was 1.05, 0.82, 0.78 and 0.89 for
 154 specimen 1-4 respectively.

$$A_{ratio} = \frac{\text{Capillary Surface Area}}{\text{Villi Surface Area}} \quad (4)$$

155 3.2. Diffusion Analyses

156 An example of the distributions of the concentration and oxygen flux are provided in
 157 Figure 3 for each specimen. The vasculo-syncytial membranes, as expected, showed larger
 158 fluxes when compared to thicker areas of the tissue due to the small diffusion distances.

159 Parametric studies of the oxygen concentrations in the membrane and capillary surfaces
 160 showed no difference in the results when the driving oxygen gradient remained constant.
 161 However, the increase of the gradient had a profound effect in both the total oxygen flux
 162 and concentration magnitudes. Interestingly, the capillary boundaries that faced towards the
 163 center of the villi (opposite to the villous membrane) received very little oxygen (see Figure
 164 3).

165 The oxygen flux magnitude was averaged (see Appendix A for details on local averaging)
 166 along different membrane thicknesses and was found to be inversely proportional to the
 167 villous membrane thickness (Figure 4). It can be recognized that, as expected, the maximum
 168 oxygen flux occurs at the thinnest barriers and the minimum at the thicker areas. The

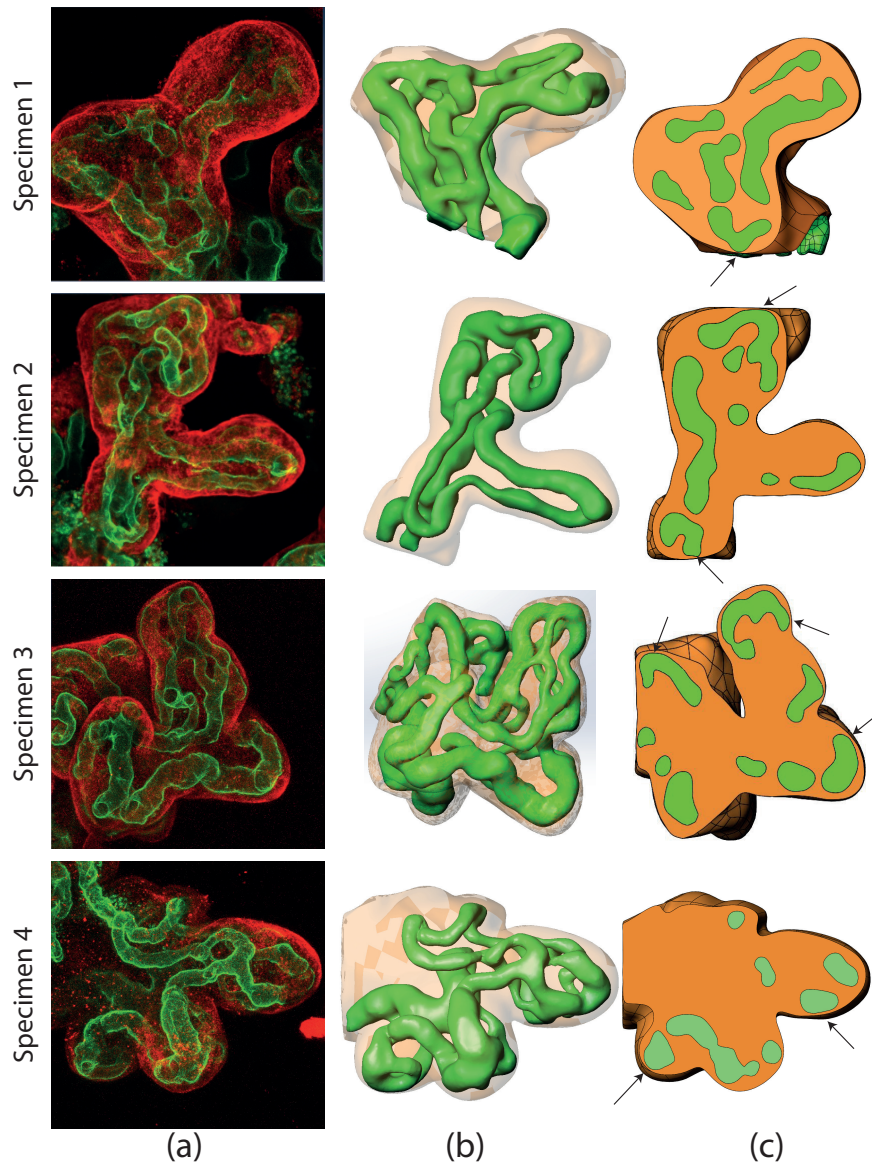


Figure 2: Geometrical reconstructions of the terminal villi and its capillary bed for all specimens. (a) 2D CLSM stacks, (b) Three-dimensional reconstructions and (c) Cut view showing different locations of vasculo-syncytial membranes.

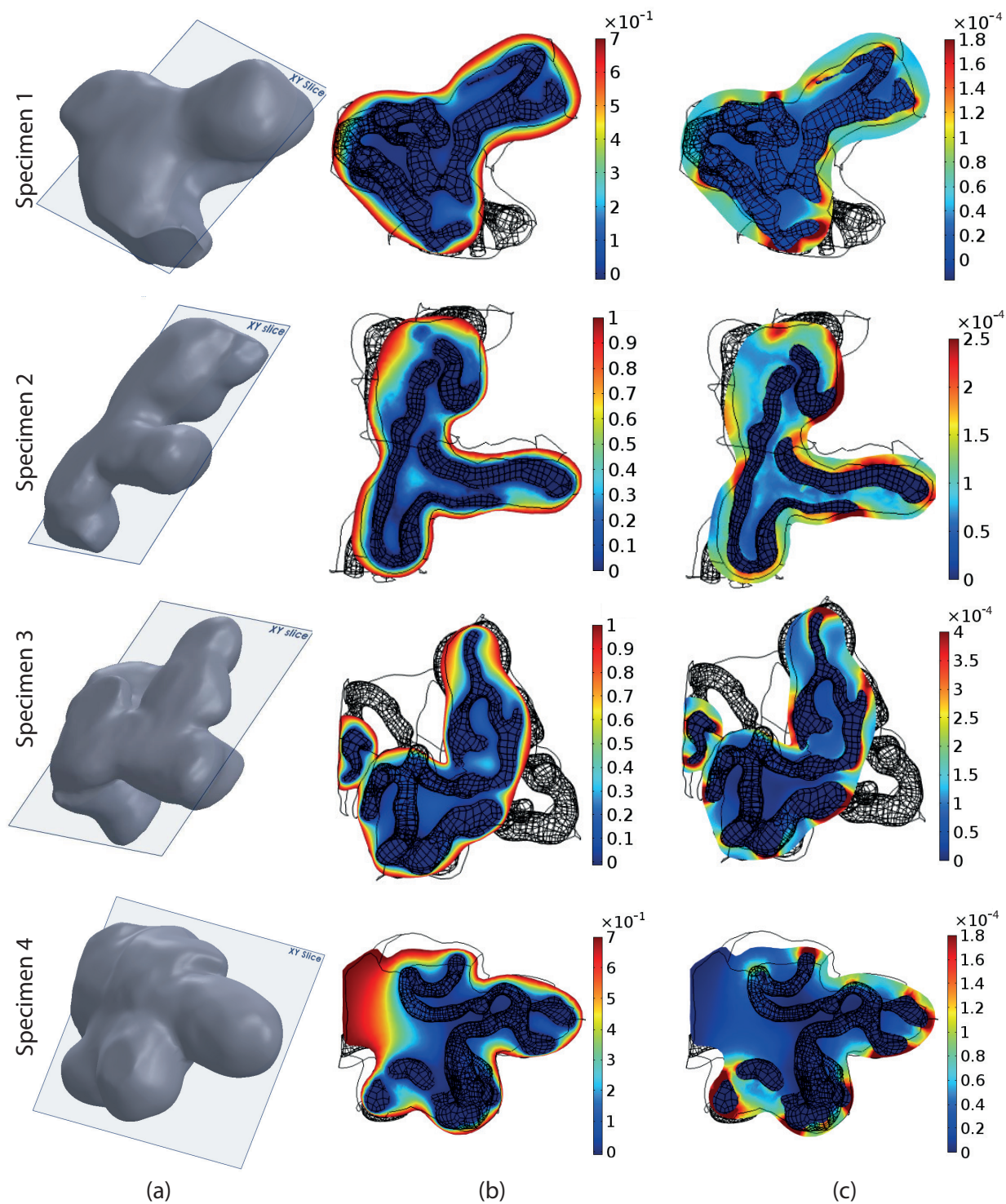


Figure 3: Distribution maps in a model with $D = 1.62 \cdot 10^{-9} \text{ m}^2/\text{s}$. (a) Representative xy slice, (b) Concentration [mol/m^3] and (c) Flux magnitude [$\text{mol}/\text{m}^2 \cdot \text{s}$] distributions.

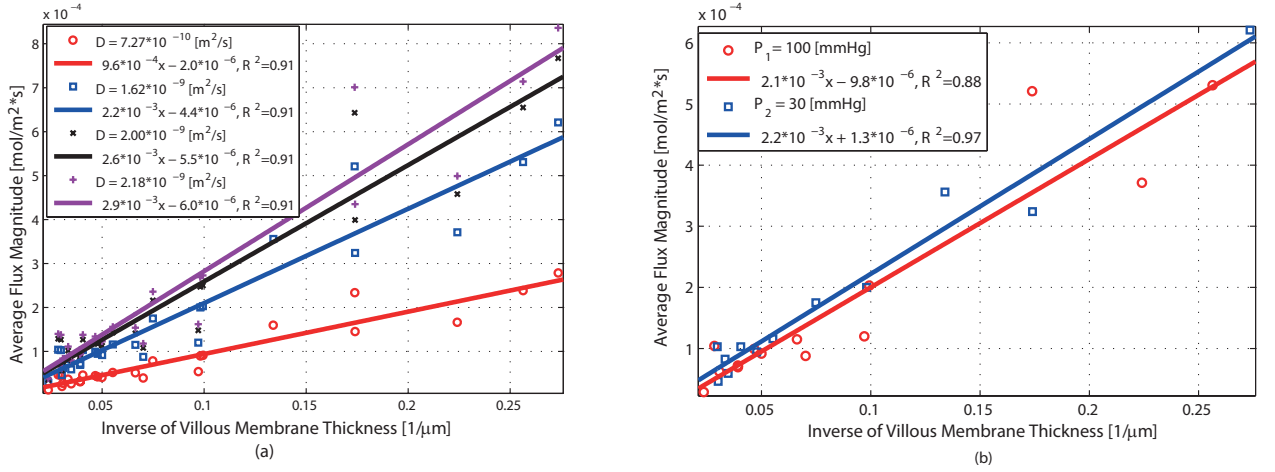


Figure 4: Average oxygen flux magnitude [mol/m²·s] vs. villous membrane thickness [μm]. (a) Results of the parametric study for the diffusion coefficient, D , and (b) Comparison between the different fixation pressures, P .

169 diffusion coefficient has a significant effect on the rate and amount of oxygen that diffuses
 170 especially in the smallest distances.

171 The efficiency E , Eq. 3, of the terminal villi was $1.54 \cdot 10^{-4}$, $2.89 \cdot 10^{-4}$, $3.20 \cdot 10^{-4}$ and
 172 $1.90 \cdot 10^{-4}$ for specimens 1-4 respectively (with $C_{villi} = 1 \cdot 10^{-9} \text{ mol/m}^3$).

173 4. Discussion

174 Research on the human placenta is challenging, mainly due to ethical considerations, the
 175 inaccessibility of the living organ, and the manipulation of the *ex vivo* tissue. Furthermore,
 176 there is considerable interspecies variation [31] which complicates the interpretation of animal
 177 studies. On the other hand, mathematical models are limited by the geometrical complexity
 178 of the system and its solute patterns [2, 20, 32]. As a consequence, the effect of certain
 179 parameters on the transport capacity and efficiency of the human placenta have not been
 180 effectively studied, leading to an urgent need for new research techniques. The current study
 181 was designed to assess the capabilities of specimen-specific FE analysis as an investigative
 182 tool for the human terminal villi.

183 Three-dimensional reconstructions showed different types of capillary loops and non-
 184 uniform capillary diameters, a feature that has been previously reported and referred to as
 185 sinusoids [30, 33]. It has been previously suggested that mechanical forces, *e. g.* pressure
 186 gradients, are responsible for sculpting these capillaries [1]. However, further research is still
 187 needed to clarify this idea and its effect on the fetal blood flow and diffusion capacity of the
 188 human placenta.

189 Even though there is a significant amount of data in the literature regarding the geometrical
 190 parameters of the villous components, most of them were calculated in a whole placenta
 191 rather than in a single terminal villus [3-5, 34-37]. Few works have calculated geometrical
 192 parameters such as volume fractions or surface area fractions in the terminal villus [24, 38, 39];

193 in agreement with Karimu et al. [39], averaged capillary to villi volume and area fractions
194 were found to decrease with the fixation pressure. Both fractions were at least half of those
195 reported by Karimu et al. [39] but in agreement with the lower values reported by Burton
196 et al. [24]. The exact source of this discrepancy is unknown, but the different techniques
197 for the estimation of parameters and the small sample cohort are believed to be related.
198 Interestingly, some studies found the surface area of the villi to be bigger than that of the
199 capillaries [17, 36, 40, 41], while others reported the opposite [3, 5, 24, 42]; in this work
200 both cases were found. Terminal villi geometries are variable within a single placenta and
201 between villi [31] and therefore it is no surprise to find the different cases to be reported.
202 The surface area ratio may be related to the amount of dilation of specific segments rather
203 than to external factors since.

204 Most existing works used a morphometric approach to model 2D oxygen transport, where
205 structural quantities were estimated by sectioning fixed sampled tissue and combined with
206 physicochemical data. Many different aspects and scenarios of placental exchange have
207 been studied using this technique [3, 5, 15–18, 43, 44]. However, 2D geometries cannot
208 provide a full quantitative analysis of a 3D system because of inevitable geometrical and
209 mathematical simplifications. A different approach is to simplify the placental geometry to
210 allow for a numerical solution of a more complex scenario [21, 22]; a study done by Serov et
211 al. [20] modeled a complex scenario (including maternal and fetal bloodstreams, membrane
212 permeability and oxygen-hemoglobin dissociation curve) but simplified the terminal villi
213 geometry to parallel tubes with constant diameters. This geometrical representation disables
214 any function - structure relation, meaning that the different blood flow patterns (concurrent,
215 counter-current or any other organization) provide the same results. To the best of the
216 authors' knowledge this is the only work that applies FE analysis to the problem of oxygen
217 transport across fully 3D terminal villi in the human placenta.

218 To obtain a reliable model, the geometry and the oxygen transport problem should
219 describe as closely as possible the *in vivo* state. Here, the focus was initially on an accurate
220 3D reconstruction of randomly selected human placental terminal villi while a simplified
221 mathematical description of the oxygen transport problem is solved. In this way, the FE
222 capabilities to provide fast and accurate results can be tested. Figure 4 summarizes the
223 importance of the membrane thickness on the total oxygen flux; not surprisingly larger
224 diffusion coefficients led to higher oxygen transport fluxes. This behavior was predictable
225 from Fick's law of diffusion where one can estimate the effect of the different D on the flux,
226 for a simplified model, to be $D \cdot \Delta C / h$ (h being the membrane thickness). Interestingly, the
227 specimens which were perfused at the lower pressure (specimens 3 and 4) yielded larger
228 values of oxygen flux in the thicker areas while those fixed at the higher pressure (specimens
229 1 and 2) transported larger amounts of oxygen in the thinner areas (Figure 4). It might be
230 that the higher fixation pressure leads to more variability in the membrane thickness while
231 the lower pressures resulted in a more even but thicker membrane. The surroundings of
232 the vasculo-syncytial membranes appear to have an effect on the oxygen flux through them
233 which does not only depend on a specific diffusion thickness. This effect can only be seen
234 and investigated using a realistic 3D model of the terminal villi.

235 The concentration and flux distributions showed that while the vasculo-syncytial mem-

236 branes transported large amounts of oxygen, the boundaries that faced towards the center
237 of the specimen were exposed to little oxygen. This phenomenon supports the previously
238 reported study on diffusional screening[2], whereby some capillary sections are shielded from
239 receiving oxygen by others. An explanation could be that oxygen may diffuse out from the
240 deeper capillary surfaces to supply the cells of the stromal core, but only a full computational
241 model that includes the fetal bloodstream, the active transport and the trophoblast membrane
242 oxygen consumption could clarify this phenomenon.

243 In the present study, the geometrical reconstructions largely depend on the staining quality
244 of the tissues and the resolution of the CLSM. As a consequence, human interpretation is
245 needed to remove imaging artifacts, which can sometimes be challenging. Currently, it is
246 impossible to completely automate this methodology because manual cleaning is obligatory
247 to define unclear boundaries and obtain smooth models. Additionally, the fetal blood
248 pressure in the *in vivo* human placenta is estimated to be about 50 mmHg [24], such
249 that the fixation pressures may have represented the maximum and minimum fetal blood
250 pressures. Therefore, the geometrical results may be overestimating or underestimating the
251 real geometries. Another limitation is the number of terminal villi that can be analyzed
252 simultaneously; a large number of villi such as in the work of Gill et al. [2] cannot be
253 reconstructed altogether due to resolution problems. However, the presented methodology
254 enables the different geometries to be deeply analyzed and the 3D geometry-function relation
255 to be better understood with a more automatic approach and less user dependency than the
256 one proposed by Gill et al. [2]. Finally, there are limitations associated with the difficulty
257 to experimentally validate the results. Validations to support oxygen transport studies are
258 challenging since the experimental conditions, such as the concentration of oxygen, culture
259 medium and type of matrix, must be carefully adjusted [45].

260 Despite these limitations, CLSM 3D reconstructions together with FE models have
261 the potential to become a valuable tool for placenta related research. The benefit of the
262 proposed methodology is its application in simulation-based research aimed to serve as a
263 basis for analyzing the transport capacity of human placentae. There is ongoing work to
264 experimentally validate and improve the FE models to more complex but realistic scenarios
265 where the fetal bloodstream and active transport are incorporated.

266 **Appendix A. Local Averaging**

267 Finite element analyses are advantageous because their outcome is in a detailed form,
268 e.g. values on every point. Therefore, to extract results either on a line, surface or volume
269 an averaging method is needed.

270 COMSOL Multiphysics automatically defines a line when selecting two points. For the
271 diffusive flux magnitude reported in this study, random lines connecting the fetal capillary and
272 the outer surface of the villous membrane representing the membrane thickness, were created.
273 The flux was then averaged by a standard numerical integration method (quadrature) as
274 follows:

$$\frac{\int_a^b f(x)dx}{b-a} \quad (\text{A.1})$$

275 where $f(x)$ is the flux at each point x and a, b are the two extreme points of the line. This is
 276 the default averaging method of COMSOL Multiphysics which is implemented by the ‘Line
 277 Averaging’ command under the Results section.

278 References

- 279 [1] Burton GJ, Woods AW, Jauniaux E, Kingdom JCP. Rheological and Physiological Consequences of
 280 Conversion of the Maternal Spiral Arteries for Uteroplacental Blood Flow during Human Pregnancy.
 281 *Placenta* 2009;30(6):473–82.
- 282 [2] Gill JS, Salafia CM, Grebenkov D, Vvedensky DD. Modeling Oxygen Transport in Human Placental
 283 Terminal Villi. *Journal of Theoretical Biology* 2011;291(0):33–41.
- 284 [3] Ansari T, Fenlon S, Pasha S, O’Neill B, Gillan J, Green C, et al. Morphometric Assessment of the
 285 Oxygen Diffusion Conductance in Placentae from Pregnancies Complicated by Intra-Uterine Growth
 286 Restriction. *Placenta* 2003;24(6):618–26.
- 287 [4] Mayhew TM, Sisley I. Quantitative Studies on the Villi, Trophoblast and Intervillous Pores of Placentae
 288 from Women with Well-controlled Diabetes Mellitus. *Placenta* 1998;19(5–6):371–7.
- 289 [5] Mayhew TH, Joy CF, Haas JD. Structure-Function Correlation in the Human Placenta, the Morpho-
 290 metric Diffusing Capacity for Oxygen at Full. *Journal of Anatomy* 1984;139(4):691–708.
- 291 [6] Leiser R, Krebs C, Ebert B, Dantzer V. Placental Vascular Corrosion Cast Studies: A Comparison
 292 between Ruminants and Humans. *Microsc Res Tech* 1997;38:76–87.
- 293 [7] Burton G. The fine structure of the human placental villus as revealed by scanning electron microscopy.
 294 *Scanning Microscopy* 1987;1:1811–28.
- 295 [8] Langheinrich AC, Vormann S, Seidenstücker J, Kampschulte M, Bohle RM, Wienhard J, et al. Quantitative
 296 3D Micro-CT Imaging of the Human Feto-placental Vasculature in Intrauterine Growth Restriction.
 297 *Placenta* 2008;29(11):937–41.
- 298 [9] Langheinrich AC, Wienhard J, Vormann S, Hau B, Bohle RM, Zygmunt M. Analysis of the Fetal
 299 Placental Vascular Tree by X-ray Micro-Computed Tomography. *Placenta* 2004;25(1):95–100.
- 300 [10] Lisman BAM, van den Hoff MJB, Boer K, Bleker OP, van Groningen K, Exalto N. The Architecture of
 301 First Trimester Chorionic Villous Vascularization: A Confocal Laser Scanning Microscopical Study.
 302 *Human Reproduction* 2007;22(8):2254–60.
- 303 [11] Jirkovská M. Spatial Arrangement of the Microvascular Bed in the Human Placenta. *Androl Gynecol:*
 304 *Curr Res* 2013;1:4.
- 305 [12] Resta L, Capobianco C, Marzullo A, Piscitelli D, Sanguedolce F, Schena FP, et al. Confocal Laser
 306 Scanning Microscope Study of Terminal Villi Vessels in Normal Term and Pre-eclamptic Placentas.
 307 *Placenta* 2006;27(6–7):735–9.
- 308 [13] Kirschbaym T, Shapiro N. A Mathematical Model of Placental Oxygen Transfer. *Journal of Theoretical*
 309 *Biology* 1969;25:380–402.
- 310 [14] Weibel ER. Morphometric Estimation of Pulmonary Diffusion Capacity: I. Model and Method.
 311 *Respiration Physiology* 1971;11(1):54–75.
- 312 [15] Bacon BJ, Gilbert RD, Kaufmann P, Smith A, Trevino FT, Longo LD. Placental Anatomy and Diffusing
 313 Capacity in Guinea Pigs following long-term Maternal Hypoxia. *Placenta* 1984;5:475–88.
- 314 [16] Longo L, Ching K. Placental Diffusing Capacity for Carbon Monoxide and Oxygen in Unanesthetized
 315 Sheep. *Journal of Applied Physiology* 1977;43:885–93.
- 316 [17] Mayhew TM, Jackson MR, Haas JD. Microscopical Morphology of the Human Placenta and Its Effects
 317 on Oxygen Diffusion: a Morphometric Model. *Placenta* 1986;7:121–31.

- 318 [18] Reshetnikova OS, Burton GJ, Teleshova OV. Placental Histomorphometry and Morphometric Diffusing
319 Capacity of the Villous Membrane in Pregnancies Complicated by Maternal Iron-deficiency Anemia.
320 American Journal of Obstetrics and Gynecology 1995;173(3):724–7.
- 321 [19] Chernyavsky IL, Leach L, Dryden IL, Jensen OE. Transport in the Placenta: Homogenizing Haemody-
322 namics in a Disordered Medium. Phil Trans R Soc A 2011;369(4162-4182).
- 323 [20] Serov AS, Salafia C, Brownbill P, Grebenkov DS, Filoche M. Optimal Villi Density for Maximal Oxygen
324 Uptake in the Human Placenta. Journal of Theoretical Biology 2015;368:133–44.
- 325 [21] Costa A, Costantino ML, Fumero R. Oxygen Exchange Mechanisms in the Human Placenta: Mathe-
326 matical Modelling and Simulation. Journal of Biomedical Engineering 1992;14:385–9.
- 327 [22] Gordon Z, Eytan O, Jaffa A, Elad D. Fetal Blood Flow in Branching Models of the Chorionic Arterial
328 Vasculature. Annals of the New York Academy of Sciences 2007;:250–65.
- 329 [23] Serov AS, Salafia C, Grebenkov DS, Filoche M. The Role of Morphology in Mathematical Models of
330 Placental Gas Exchange. J Appl Physiol 2016;120:17–28.
- 331 [24] Burton GJ, Ingram SC, Palmer ME. The Influence of Mode of Fixation on Morphometrical Data
332 Derived from Terminal Villi in the Human Placenta at Term: A Comparison of Immersion and Perfusion
333 Fixation. Placenta 1987;8:37–51.
- 334 [25] Karimu AL, Burton GJ. Significance of changes in fetal perfusion pressure to factors controlling
335 angiogenesis in the human term placenta. Journal of Reproduction and Fertility 1994;102(2):447–50.
- 336 [26] Fedorov A, Beichel R, Kalpathy-Cramer J, Finet J, Fillion-Robin JC, Pujol S, et al. 3D Slicer as
337 an Image Computing Platform for the Quantitative Imaging Network. Magnetic Resonance Imaging
338 2012;30(9):1323–41.
- 339 [27] Shapiro LG, Stockman GC. Computer Vision. Prentice Hall; 2002.
- 340 [28] Lorensen WE, Cline HE. Marching Cubes: A High Resolution 3D Surface Construction Algorithm. In:
341 Proceedings of the 14th Annual Conference on Computer Graphics and Interactive Techniques. 1987, p.
342 163–9.
- 343 [29] Szabo B, Babuska I. Introduction to Finite Element Analysis: Formulation, Verification and Validation.
344 Wiley-Blackwell; 2011.
- 345 [30] Burton GJ, Tham SW. The Formation of Vasculo-Syncytial Membranes in the Human Placenta.
346 Journal of Developmental Physiology 1992;43-47.
- 347 [31] Benirschke K, Burton GJ, Baergen RN. Pathology of the Human Placenta. Springer; 2012.
- 348 [32] Chernyavsky IL, Jensen OE, Leach L. A Mathematical Model of Intervillous Blood Flow in the Human
349 Placenta. Placenta 2010;31(1):44 – 52.
- 350 [33] Jirkovská M, Kubínová L, Janáček J, Kaláb J. 3D Study of Vessels in Peripheral Placental Villi. Image
351 Analysis & Stereology 2007;26(3):165–8.
- 352 [34] Rainey A, Mayhew T. Volumes and Numbers of Intervillous Pores and Villous Domains in Placentas
353 Associated with Intrauterine Growth Restriction and/or Pre-eclampsia. Placenta 2010;31(7):602 –6.
- 354 [35] Mayhew TM. A Stereological Perspective on Placental Morphology in Normal and Complicated
355 Pregnancies. Journal of Anatomy 2009;215:77 – 90.
- 356 [36] Mayhew TM, Manwani R, Ohadike C, Wijesekara J, Baker PN. The Placenta in Pre-eclampsia and
357 Intrauterine Growth Restriction: Studies on Exchange Surface Areas, Diffusion Distances and Villous
358 Membrane Diffusive Conductances. Placenta 2007;28(2-3):233 –8.
- 359 [37] Egbor M, Ansari T, Morris N, Green C, Sibbons P. Pre-eclampsia and Fetal Growth Restriction: How
360 Morphometrically Different is the Placenta? Placenta 2006;27(6-7):727 –34.
- 361 [38] Burton GJ, Reshetnikova OS, Milovanov AP, Teleshova OV. Stereological Evaluation of Vascular
362 Adaptations in Human Placental Villi to Differing Forms of Hypoxic Stress. Placenta 1996;17(1):49 –
363 55.
- 364 [39] Karimu A, Burton G. The Effects of Maternal Vascular Pressure on the Dimensions of the Placental
365 Capillaries. British Journal of Obstetrics and Gynaecology 1994;101:57–63.
- 366 [40] Egbor M, Ansari T, Morris N, Green CJ. Morphometric Placental Villous and Vascular Abnormalities
367 in Early- and Late-onset Pre-eclampsia with and without Fetal Growth Restriction. BJOG : An
368 International Journal of Obstetrics and Gynaecology 2006;113(5):580–9.

- 369 [41] Mayhew TM, Wijesekara J, Baker PN, Ong SS. Morphometric Evidence that Villous Development
370 and Fetoplacental Angiogenesis are Compromised by Intrauterine Growth Restriction but not by
371 Pre-eclampsia. *Placenta* 2004;25(10):829–33.
- 372 [42] Burton GJ, Jauniaux E. Sonographic, Stereological and Doppler Flow Velocimetric Assessments of
373 Placental Maturity. *British Journal of Obstetrics and Gynaecology* 1995;102:818–25.
- 374 [43] Mayhew TM. Estimating Oxygen Diffusive Conductances of Gas-Exchange Systems: A Stereological
375 Approach Illustrated with the Human Placenta. *Annals of Anatomy* 2013;.
- 376 [44] Reshetnikova OS, Burton GJ, Milovanov AP. Effects of Hypobaric Hypoxia on the Fetoplacental Unit:
377 The Morphometric Diffusing Capacity of the Villous Membrane at High Altitude. *American Journal of*
378 *Obstetrics and Gynecology* 1994;171(6):1560–5.
- 379 [45] Schneider H. Oxygenation of the Placental-Fetal Unit in Humans. *Respiratory Physiology & Neurobiology*
380 2011;178(1):51–8.